INDIAN JOURNAL OF SCIENCE AND TECHNOLOGY

RESEARCH ARTICLE

Optical, Mechanical and Dielectric Characterization of 5-(3,4,5-Trimethoxybenzyl) Pyrimidine-2,4-Diamine (Trimethoprim- An Antibiotic Drug) Single Crystal

Samuel Robinson Jebas[1]*, **J Anantha Meena Geetha**[2]

1 Associate Professor, PG and Research Department of Physics, Kamarajar Government Arts College (Affiliated to Manonmaniam Sundaranar University, Abishekapatti, Tirunelveli-627012), Surandai, Tenkasi Dt, 627859, Tamilnadu, India
2 Research Scholar (21211062132002), PG and Research Department of Physics, Kamarajar Government Arts College (Affiliated to Manonmaniam Sundaranar University, Abishekapatti, Tirunelveli-627012), Surandai, Tenkasi Dt, 627859, Tamilnadu, India

OPEN ACCESS

Received: 25-04-2024
Accepted: 17-06-2024
Published: 22-07-2024

Citation: Jebas SR, Geetha JAM (2024) Optical, Mechanical and Dielectric Characterization of 5-(3,4,5-Trimethoxybenzyl) Pyrimidine-2,4-Diamine (Trimethoprim- An Antibiotic Drug) Single Crystal. Indian Journal of Science and Technology 17(28): 2914-2923. https://doi.org/10.17485/IJST/v17i28.1393

* **Corresponding author**.

jebas2@gmail.com

Funding: None

Competing Interests: None

Published By Indian Society for Education and Environment (iSee)

ISSN
Print: 0974-6846
Electronic: 0974-5645

Abstract

Objectives: To evaluate the optical properties of the trimethoprim (TMP) single crystal. **Methods:** 5-(3, 4, 5- trimethoxybenzyl) pyrimidine-2-4-diamine known as trimethoprim (TMP), a single crystal is a well-known antibiotic drug, was grown by the slow evaporation method. **Findings:** The TMP unit cell parameters were confirmed by single crystal X-ray diffraction. Functional groups of TMP crystal was confirmed by Fourier transform infrared spectral analysis. The optical spectrum shows the wide transparency window of TMP which is the prerequisite for NLO material. The band gap is calculated as 4.10 eV from Tauc's plot. The various optical constants like extinction coefficient, refractive index and reflectance were calculated from the transmittance spectrum data. The optical and electrical parameters like optical conductivity, electrical conductivity and susceptibility of the single crystal of TMP were determined from the UV spectrum. The fluorescence spectrum shows the presence of a sharp intense peak at 690 nm indicates red emission and a weak peak observed at 480 nm indicates blue emission. The Vickers hardness study shows the grown crystal belongs to the soft type single crystal with Meyer's index (n) of 2. The yield strength of the crystal was calculated. Dielectric constant and dielectric loss are measured as a function of frequency. The laser damage threshold of the TMP crystal was measured using an Nd: YAG laser with a wavelength of 1064 nm. **Novelty:** The various studies show that the TMP crystal possesses excellent optical properties and can be used for opto-electronics device fabrication.

Keywords: Unit cell; Transmittance; Emission; Hardness; Dielectric constant and loss

1 Introduction

Crystals play an important role in semiconductors and optoelectronics, which study the potential and relevance of crystals in many technological applications such as photonics and optoelectronics. Organic materials are expanding as a result of their exciting nonlinear efforts in optical applications. Optical applications depend upon physical characteristics such as refractive index, birefringence, thermal stability, and physicochemical properties[1]. Many of these applications require materials with strong second-order optical nonlinearity, high optical transmittance with low cut-off wavelength, high laser damage threshold value, and easy growth with big dimensions. The development of new types of optical crystals with desirable physical and chemical properties is critical in optoelectronics, photonics laser processing, and other applications[2].

This enables the creation of materials with specialized properties that may be tuned for specific uses. The 5-(3, 4, 5-trimethoxybenzyl) pyrimidine-2,4-diamine (TMP) is a well-known antifolate drug used mainly in the treatment of urinary tract infections. Several multi-component crystal phases of trimethoprim include cocrystals, some of which have been reported including salts with mefenamic acid[3], sulfamethoxazole[4], and malic acid[5]. Pharmaceutical compounds and conformers could be formed due to non-covalent intermolecular interactions such as vander waals and hydrogen bonds[6]. The literature survey revealed the biological and co-crystal importance of trimethoprim but only a few studies have been reported related to the optical importance of trimethoprim. Since no studies were found to be reported on the optical, mechanical, and dielectric properties of this well-known drug, aroused by curiosity we have reported here the optical properties, mechanical behavior, and dielectric properties of the drug trimethoprim. We hope the article will serve as a reference for future experimental and analytical efforts with single crystals to improve their mechanical behavior and optoelectronic qualities, with a final objective of advancing optoelectronic technology.

2 Methodology

5-(3, 4, 5- trimethoxybenzyl) pyrimidine-2,4-diamine was dissolved in 20 ml ethanol. The clear solution obtained was allowed to evaporate slowly. Pale yellow crystals were harvested after a week. Figure 1 shows the grown crystal. The chemical structure of the grown crystal is shown in Figure 2.

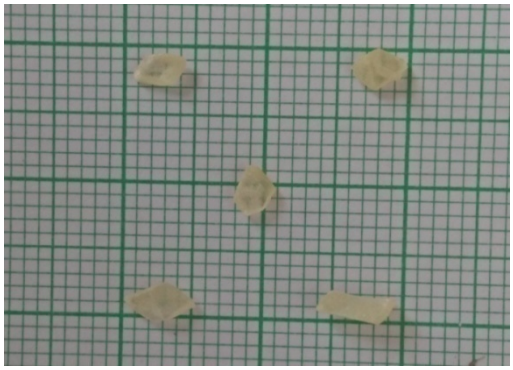

Fig 1. Crystals of TMP

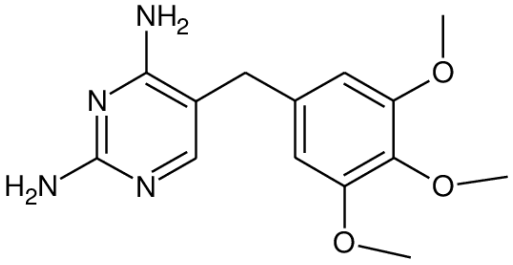

Fig 2. Chemical structure of TMP

3 Result and Discussion

3.1. Single Crystal X-Ray Diffraction

Single crystal X-ray diffraction (XRD) is a non-destructive tool to analyze the crystal structure of compounds, which can be grown as single crystals. XRD is employed for finding unit cell parameters and crystal systems. The grown TMP single crystal was subjected to single-crystal X-ray diffraction analysis using a BRUKER Q8 QUEST Duo X-ray diffractometer to determine the cell parameters. The crystal is triclinic with the cell parameters of a = 7.76 (3) Å, b = 10.07 (3) Å, c = 18.36 (7) Å, α = 85.57(11) °, = 89.39(11) °, γ = 68.48(10) °. The calculated volume of 1329 (13) Å.

3.2. FTIR Analysis

Fourier transform infrared spectrum of TMP single crystal was recorded in a Perkin-Elmer Spectrometer in the range of 4000 cm-1 to 400 cm-1. The purpose of the FTIR study is to confirm the presence of functional groups. Strong NH stretching bands in the spectra of aromatic amines have been assigned as in 3470.08 cm^{-1} [(7)]. The band at 2931.67 cm^{-1} is due to the C-H stretching. The band at 1977.91 cm^{-1} is due to the C=N stretching. The peaks at 1636.04 cm^{-1} are due to NH_2 Symmetric stretching vibration [(7)]. The asymmetric CH_3 bending 1463.18 cm^{-1} methyl group. The bands at 1334.70 cm^{-1} is assigned to C-N stretching vibration. A band at 1128.78 cm^{-1} is assigned to the C-O stretching vibration. The band at 800.68 cm^{-1} is assigned to the aromatic C=C stretching vibrations [(7)]. The FT-IR spectrum of TMP is shown in Figure 3.

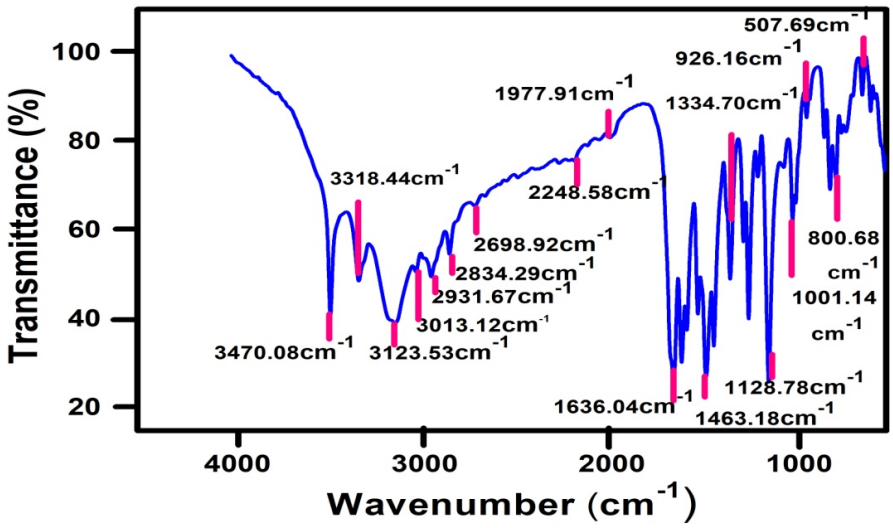

Fig 3. FTIR spectrum of TMP

3.3. UV-Visible NIR Analysis

When a UV-visible ray passes through the growing crystal, the absorption of light energy causes the electrons to move from the ground state to a higher energy state. The optical transmittance spectrum of TMP single crystal was recorded using Perkin Elmer Lambda 35 spectrophotometer in the wavelength range of 190 nm to 1100 nm. The transmittance spectrum is shown in Figure 4. The cut-off wavelength of the TMP crystal was observed at 280 nm. The spectrum reveals 98% transparency in the UV, an entirely visible range, and no major absorption, indicating that the TMP crystal is suitable for optoelectronic device construction and second harmonic generation.

3.3.1. Optical Band Gap Energy (E_g)

The optical band gap energy is proportional to the atomic and electronic band structures of the formed crystals [(8)]. Optical band gap energy is determined by their optical absorption coefficient and incident photon energy. The optical absorption coefficient

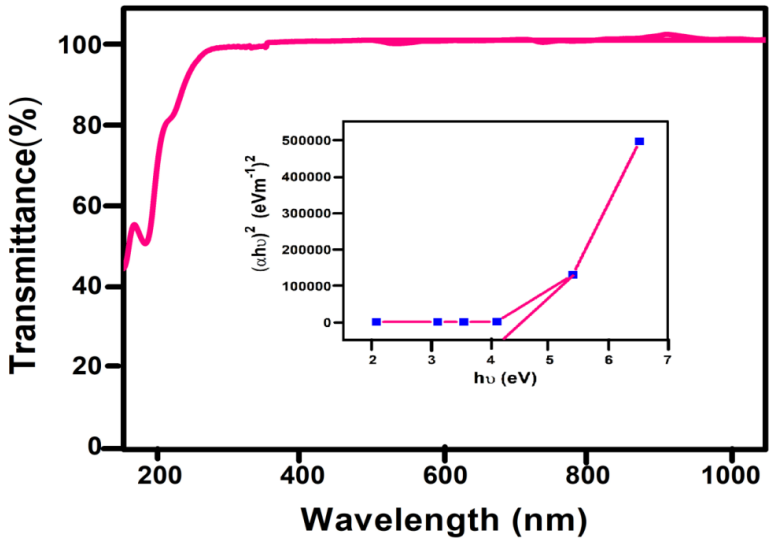

Fig 4. Optical transmittance spectrum of TMP with the plot of hυversus $(\alpha h\upsilon)^2$

(α) was calculated using equation [9].

$$\alpha = \left(\frac{2.3036}{t}\right) log\frac{1}{T} m^{-1}$$

Where T is the transmittance and t is the thickness of the crystal. The optical band gap energy (E_g) is related to absorption coefficient (α) and photon energy (hυ) through the Tauc's relation [10]

$$\alpha h\upsilon = A(h\upsilon - E_g)^{1/2}$$

Where A is optical constant, E_g is the optical band gap energy, h is the Planck's constant and υ is the frequency of the incident photon. Experimentally, the optical band gap (E_g) of TMP crystal was found to be 4.10 eV from the Tauc's plot. The value of the wide band gap indicates its suitability for photoconductivity applications. The band gap of the grown TMP crystal was computed by plotting hυ versus $(\alpha h\upsilon)^2$ and is shown in Figure 4. According to the Plank-Einstein relation, the energy of a photon (E) is proportional to its frequency, and hence theoretically, the optical band-gap energy of a TMP crystal can be calculated using the following relations,

$$E = \frac{hc}{\lambda}$$

Where λ is the lower cut-off wavelength (280 nm). The band gap of the grown crystal is found to be 4.42 eV.

3.3.2. Determination of Optical Constants

The total energy outflow of the applied electromagnetic radiation when it transmits throughout the material is calculated by the extinction coefficient (K) which is interrelated to the absorption expression [11],

$$K = \frac{\alpha\lambda}{4\pi}$$

Where α is the optical absorption coefficient, λ is the wavelength. The extinction coefficient values can be calculated from the UV-visible spectrum. The plot of wavelength versus extinction coefficient (K) and refractive index is shown in Figure 5. The reflectance refers to the portion of an incident light which is reflected when it is incident on the surface of the crystal. The reflectance (R) in terms of absorption coefficient (α) and the thickness of the crystal (t) can be determined using the below

relation [12],

$$R = 1 \pm \frac{\sqrt{1 - exp(-\alpha t) + exp(\alpha t)}}{1 + exp(-\alpha t)}$$

The refractive index is the measure of the speed of light. It is a key parameter for optical device design. The measurement of refractive index n can be determined from reflectance data using the equation [12],

$$n = \frac{-(R+1) \pm \sqrt{-3R^2 + 10R - 3}}{2(R-1)}$$

The calculated refractive index (n) value using the above equations for the grown TMP is 2.72. The refractive index can be determined from the reflectance (R) data using,

$$R = \frac{(n-1)^2}{(n+1)^2}$$

The calculated value of reflectance (R) is 0.2134. Reflectance as a function of wavelength is graphically illustrated in Figure 6.

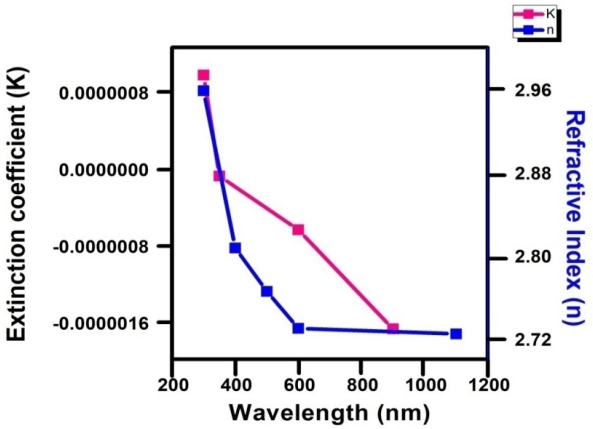

Fig 5. Wave length versus K versus n of TMP

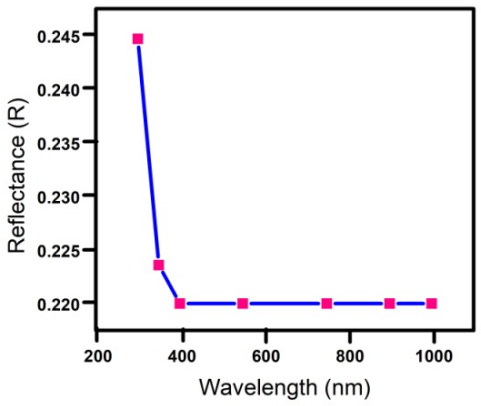

Fig 6. Wavelength versus R of TMP

3.3.3. Optical Conductivity

Optical conductivity explains charge distribution and the formation of induced and electronic states in the material. The equationis used to compute optical conductivity[12].

$$\sigma_{op} = \frac{\alpha nc}{4\pi}$$

Where c is the velocity of light, α is the optical absorption coefficient and n is the refractive index. The plot of wavelength versus optical conductivity and electrical conductivity is shown in Figure 7. The calculated optical conductivity value is 0.02670 for TMP. The higher value of optical conductivity (10^9-10^{12}) shows very good photo response of the TMP crystal. It is indicated that TMP exhibits a good optical response.

3.3.4. Electrical Conductivity

Electrical conductivity refers to how easily an electric charge or heat passes through a material. The value of the electrical conductivity of a material is related to the optical conductivity value of the crystal using the following equation,

$$\sigma_e = \frac{2\lambda\sigma_{op}}{\alpha}$$

The plot of photon energy versus optical conductivity and electrical conductivity is shown in Figure 7. The optical conductivity of TMP increases with increase in photon energy as shown in the Figure 7, indicates the very good optical response of the material. The calculated electrical conductivity value is 854.9347 for TMP.

3.3.5. Electric Susceptibility

The electric susceptibility (χ_c) values are estimated using the calculated extinction coefficient and refractive index values of TMP crystal by the below relation [12],

$\varepsilon_r = \varepsilon_0 + 4\pi\chi_c = n^2 - k^2$

$\chi_c = n^2 - k^2 - \varepsilon_0/4\pi$

Where ε_o is the permittivity in free space. The complex dielectric constant is given by $\varepsilon_{c.}$ The real and imaginary part of the dielectric constant from the extinction coefficient is given as.

$\varepsilon_c = \varepsilon_r + \varepsilon_i$

$\varepsilon_r = n^2 - k^2$

$\varepsilon_i = 2nk$

Where $\varepsilon_r$and ε_i are real and imaginary parts of dielectric constant. The electric susceptibility is calculated as χ_c = 5.8214. The real ε_r and imaginary ε_i values of dielectric constant are 7.4158 and 3.0991*10^{-6}.

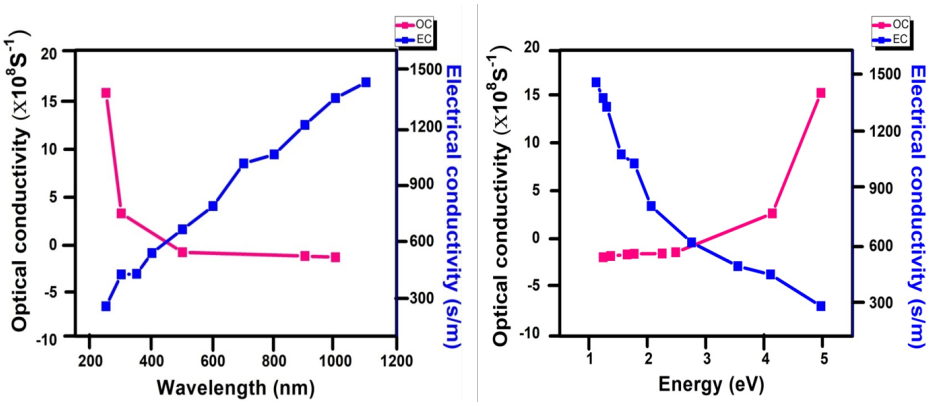

Fig 7. (a) Plot of λ versus σ_{op} & σ_e of TMP (b). Plot of Energy

3.4. *Fluorescence Analysis*

The electronic structure of materials can be examined contactlessly and nondestructively using the fluorescence spectrum. It is the light that a substance spontaneously emits when it is excited optically[13]. The excitation and emission spectrum of

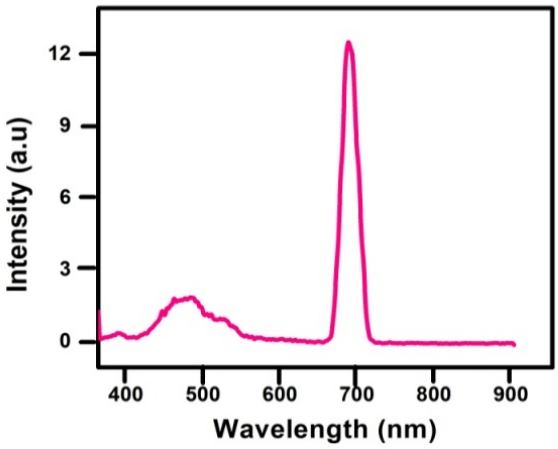

Fig 8. Emission spectrum of TMP

grown TMP crystal was recorded in the range of 260 nm to 900 nm by means of the Perkin Elmer model LS-45 fluorescence spectrometer. Figure 8 shows the emission spectrum of TMP. The TMP crystal was excited at 360 nm. The emission spectrum reveals that the TMP crystal shows the presence of a sharp intense peak at 690 nm, red emission, and a weak peak observed at 480 nm blue emission. The higher wavelength range shows an increasing drop in intensity. The presence of crystal imperfections is indicated by the emission band. The presence of a single sharp peak shows good crystalline perfection [14].

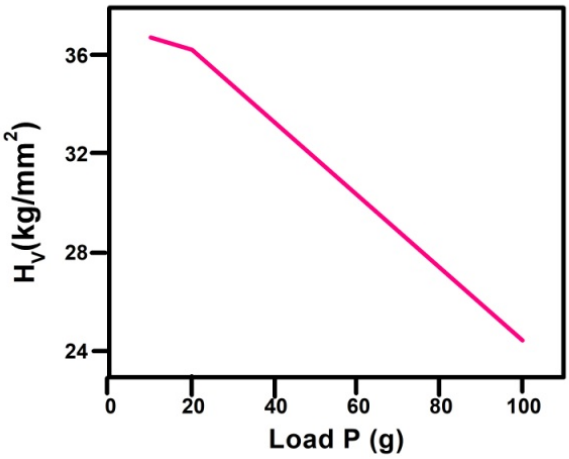

Fig 9. Load P versus hardness number H_v

3.5. Microhardness Analysis

Microhardness study was carried out in the TMP crystal for various loads from 10-100g with a constant time of indentation (10s) using a Shimadzu MHV-G21 microhardness tester fitted with diamond pyramidal indenter. The diagonal length was measured for each instance, and the average was determined. The Vickers hardness parameter (H_v) is calculated using the formula [15]

$$H_v = \frac{1.8544\, x\, P}{d^2}\, kg/mm^2$$

Where P is the applied load and d is the average diagonal length of indentation. For an applied load above 100g, the crystal begins to crack. A graph was plotted between H_v versus load (P) as shown in Figure 9. This shows that the hardness decreases with the increase of load (ISE). Meyer's index number was calculated from Meyer's law which relates the load and indentation diagonal length as [15]

$P = A=kd^n$ Where A is an arbitrary constant

$\log P = \log K + n \log d$

Here, K, is the material constant, and 'n' is the Meyer's index (or) work hardening coefficient, which characterizes the material category. Figure 10 shows the plot of log P versus log d fitting data using least-squares fit method and the value of n was found to be 2. In the present study, the values of the work hardening coefficient of the grown crystals are greater than 1.6 and hence the grown crystals of this work belong to the soft material and hence they will allow the light to pass through easily [16].

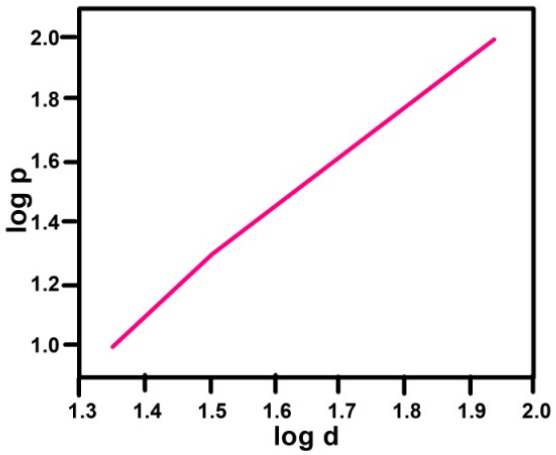

Fig 10. Log D versus log P

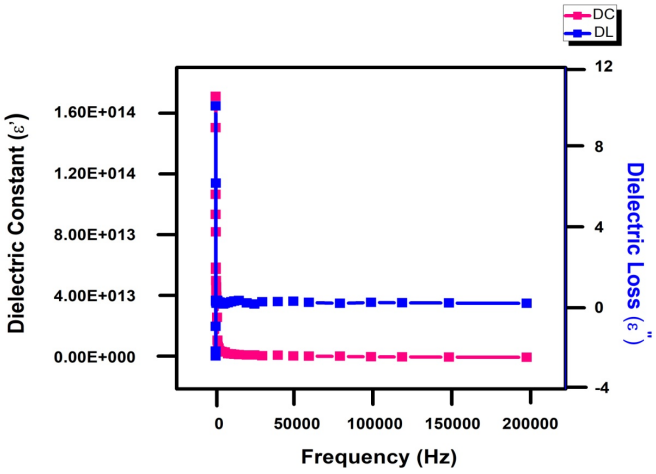

Fig 11. Variation of dielectric constant anddielectric loss with frequency

3.6. *Dielectric Analysis*

The dielectric studies on TMP crystal have been carried out using Jognic's Model 2816B LCRZ Meter. The dielectric constant of the crystal has been measured from an LCRZ meter. The presence of all polarizations, including space charge, orientation, and

electric and ionic polarizations, can be responsible for the high dielectric constant value at low frequencies[17]. The material absorbs the electrical energy, which then dissipates as heat. This dissipation of energy is called dielectric loss[18]. The plot of frequency versus dielectric constant and dielectric loss is shown in Figure 11. The dielectric loss of the crystal has been calculated using the equation, $\varepsilon' = \varepsilon \tan \delta$, Where, ε is the dielectric constant tan δ is the dispersion power factor. Due to its low dielectric loss and dielectric constant at high frequencies, this material is very useful in optical applications[19].

3.7. Laser Damage Threshold Analysis

Laser damage threshold analysis was used to assess optical crystals' capacity to tolerate laser irradiation[20]. The laser damage threshold (LDT) value is an important requirement for nonlinear optics and laser applications since it represents the maximum performance of the optical device[21]. The LDT result is primarily determined by several characteristics, including pulse width, laser wavelength, repetition rate, sample surface quality, energy, irradiance, beam size and beam placement. The LDT of the grown TMP single crystal was investigated by using Nd: YAG laser at the wavelength of 1064 nm. The pulse repetition rate and pulse width of 10 HZ and 6 ns were used for the laser damage threshold measurement. The crystal was placed at the focus of a biconvex lens (the focal length of 10 cm). The surface damage threshold of the grown crystal was calculated using the relation,

$$Power\ density\ (Pd) = \frac{E}{\tau\pi(\omega_o)^2}$$

Where E is the input pulse energy (mJ) of the laser beam when microscopic damage appeared, τ is the pulse width (ns) and ω_o is the radius of the beam waist. The laser damage threshold value was found to be 64 mJ (7.4 w/m^2) or (74 Gw/cm^2). The laser-induced damage occurs in the crystal due to its optical behavior, material defects, impurities, and surface roughness behavior. However, the direct comparison of LDT results is not accurate, because of the various testing conditions like wavelength, pulse width.

4 Conclusion

The pale yellow crystal of 5-(3, 4, 5-trimethoxybenzyl) pyrimidine-2,4-diamine (TMP) was grown by the slow evaporation method. The single-crystal XRD diffraction studies show that the grown crystal belongs to a triclinic crystal system. Various functional groups present in the TMP single crystal was identified by FTIR spectral measurements. The UV-visible NIR transmittance spectrum shows a lower cut-off wavelength of 280 nm. The lower cut-off wavelength and very good transmittance in the UV, the entire visible region, and the near-infrared region indicate the suitability of the TMP crystal for NLO applications. The band gap energy is calculated as 4.10 eV from the tauc's plot. The optical parameters like optical conductivity, electrical conductivity, and susceptibility of the crystal TMP are calculated from the UV-visible NIR spectrum. Fluorescence spectral analysis shows the presence of a sharp intense peak at 690 nm indicates red emission and a weak peak observed at 480 nm indicates blue emission. Vickers hardness test shows the crystal belongs to soft type material. The hardness parameter includes Meyer's index that has been calculated. Dielectric measurement was carried out to analyze the dielectric constant and dielectric loss of different frequencies. The laser damage threshold value was found to be 74 Gw/cm^2. All the studies suggest that the TMP crystal can be considered for optoelectronic and photonic applications.

References

1) Mutailipu M, Zhang M, Wu H, Yang Z, Shen Y, Sun J, et al. Ba3Mg3(BO3)3F3 polymers with reversible phase trasition and high performances as ultraviolet nonlinear optical materials. *Naturet Communications*. 2018;9:3089–3098. Available from: https://doi.org/10.1038/s41467-018-05575-w.
2) Chandran S, James J, Magesh G, Prasanna M. Synthesis, crystal growth, structural, spectral, laser threshold energy and dielectricbproperties of lithium L-tartrate monohydrate crystal. *Journal of Molecular Structure*. 2020;1223:1–8. Available from: https://doi.org/10.1016/j.molstruc.2020.128988.
3) Yuliandra Y, Izadihari R, Rosaini H, Zaini E. Multicomponent crystals of mefenamic acid-tromethamine with improved dissolution rate. *Journal of Research Pharmacy*. 2019;23:988–996. Available from: https://doi.org/10.35333/jrp.2019.63.
4) Bhattacharya B, Das S, Lal G, Soni S, Ghosh A, Reddy C, et al. Screening, crystal structures and solubility studies of a series of multidrug salt hydrates and cocrystals of fenamic acids with trimethoprim and sulfamethazine. *Journal of Molecular Structure*. 2019;1199:1–10. Available from: https://doi.org/10.1016/j.molstruc.2019.127028.
5) Yuliandra Y, Hutabarat LJ, Ardila R, Octavia MD, Zaini E. Enhancing solubility and antibacterial activity using multicomponent crystals of trimethoprim and malic acid. *Pharmacy Education*. 2021;21:296–304. Available from: https://doi.org/10.46542/pe.2021.212.296304.
6) Zheng Q, Unruh DK, Hutchins KM. Cocrystallization of Trimethoprim and Solubility Enhancement via Salt Formation. *Crystal Growth Design*. 2021;21:1507–1517. Available from: https://doi.org/10.1021/acs.cgd.0c01197.
7) Bayu A, Nandiyanto D, Rosioktiani R. How to Read and Interpret FTIR Spectroscope of organic Material. *Indonesian Journal of Science and Technology*. 2019;4:97–118. Available from: http://dx.doi.org/10.17509/ijost.v4i1.15806.

8) Ramachandran K, Raja A, Mohankumar V, Pandian M, Ramasamy P. Growwth and characterization of 4-methyl-3-nitrobenzoic acid (4M3N) single crystal by using vertical transparent Bridgman-Stockbarger method for NLO applications. *Physica b: Condensed Matter*. 2019;562:82–93. Available from: https://doi.org/10.1016/j.physb.2019.03.014.
9) Senthil A, Bharanidharan T, Vennila M, Elangovan K, Muthu S. Crystal growth, Hirshfeld analysis, optical, thermal, mechanical, and third-order non-linear optical properties of Cyclohexylammonium picrate (CHAP) single crystal. *Heliyon*. 2024;10:1–19. Available from: https://doi.org/10.1016/j.heliyon.2024.e28002.
10) Karuppasamy P, Kamalesh T, Mohankumar V, Kalam A, S, Pandian MS, et al. Venugopal Rao S. Synthesis, growth, structural, optical, thermal, laser damage threshold and computational perspectives of 4-nitrophenol 4-aminobenzoic acid monohydrate (4NPABA) single crystal. *Journal of Molecular Structure*. 2019;1176:254–265. Available from: https://doi.org/10.1016/j.molstruc.2018.08.074.
11) Shalini M, Sundararajan RS, Manikandan E, Meena M, Ebinezer S, B, et al. Growth and characterization of L-Methionine Barium Bromide (LMBB) semi-organic crystal for optical limiting applications. *Optik-International Journal for Light and Electron Optics*. 2023;278:1–14. Available from: https://doi.org/10.1016/j.ijleo.2023.170705.
12) Selasteen D, F, Raj AC, S. Astudy on non-linear optical properties of Copper Sodium Tartrate single crystal for non-linear optical applications. *Indian Journal of Science and Technology*. 2021;14(2):101–112. Available from: https://doi.org/10.17485/IJST/v14i2.1561.
13) Bincy P, Srinivasan T, Ramkumar JSN, V. Structure, growth and characterization of a new naphthalene family crystal for fluorescence and third order nonlinear optical applications. *Solid State Physics*. 2019;89:85–92. Available from: https://doi.org/10.1016/j.solidstatesciences.2018.12.024.
14) Mohanraj V, Thenmozhi M, Pavithra R, Jaslin J, Christopher A, Jebamalar S, et al. Growth, structure, spectral characterization, fluorescence and thermal studies on phenyltrimethylammonium trichloro cadmiate (II) crystals. *Journal of Environmental Nanotechnology*. 2021;9:42–49. Available from: https://doi.org/10.13074/jent.2020.03.201399.
15) Jebaraj G, Sivashankar P, V. Investigations on the growth and characterization of magnesium sulfate doped L-Leucinium oxalate crystals. *Journal of Advanced Scientific Research*. 2022;13:54–63. Available from: https://doi.org/10.55218/JASR.202200000.
16) Nageshwari M, Kumari RT, Sudha C, Vinitha S, G, Caroline L, et al. Spectral, dielectric, mechanical and optical characteristics of LPDMCl single crystal for nonlinear optical applications. *Physica B: Physics of Condensed Matter*. 2020;582:411980–411981. Available from: https://doi.org/10.1016/j.physb.2019.411980.
17) Gunjan V, Jigar S, Shery J. DoE implementation for Telmisartan and hydrochlorothiazide drug-drug cocrystal synthesis to enhance phsicochemical and pharmacokinetic properties. *Journal of Applied Pharmaceutical Science*. 2023;13:67–076. Available from: https://doi.org/10.7324/JAPS.2023.90012.
18) Suharyadi E, Rahayu DI, Armitasari L, Abraha K. Influences of Zn concentration on dielectric properties of ZnxNi1-xFe2O4 magnetic nanoparticles. *Makara Journal of Science*. 2018;22:163–168. Available from: https://doi.org/10.7454/mss.v22i4.10254.
19) Synthesis, Structural and Thermal Studies of Dl-Alanine Potassium Di- Chromate Single Crystals. *Makara Journal of Science*. 2024;28(1):40–46. Available from: https://doi.org/10.7454/mss.v28i1.2233.
20) Arumugan J, Suresh N, Selvapandiyan M, Sudhakar S, Prasath M. Effect of NaCl on the properties of sulphamic acid single crystals. *Heliyon*. 2019;5:1–8. Available from: .https://doi.org/10.1016/j.heliyon.2019.e01988.
21) Karupasamy P, Pandiyan MS, Ramasamy P, Verma S. Crystal growth, structural, optical, thermal, mechanical, laser damage threshold and electrical properties of triphenylphosphine oxide 4-nitrophenol (TP4N) single crystals for nonlinear optical applications. *Optical Materials*. 2018;79:152–171. Available from: https://doi.org/10.1016/j.optmat.2018.03.041.